https://doi.org/10.1016/j.atmosres.2012.08.019

THE EFFECT OF GROUND ALTITUDE ON LIGHTNING STRIKING DISTANCE BASED ON A BI-DIRECTIONAL LEADER MODEL

Mingli Chen [1*], Xueqiang Gou [1,2] and Yaping Du [1]

[1] The Hong Kong Polytechnic University, Hong Kong, China,

[2] Northwest Normal University, Lanzhou, China

*bemlchen@polyu.edu.hk

ABSTRACT

The effect of ground altitude on lightning striking distance has been investigated based on a bi-directional leader model. The model, which is a development of that proposed originally by Mazur and Ruhnke in 1998, enables the calculation of leader channel parameters, such as leader charge density, leader current, leader potential, and lightning striking distance to flat ground. In the model, the lightning striking distance is directly related to the critical electric field in the negative streamer zone in front of the leader tip and to the leader potential. The former may vary with the ground altitude above sea level and the latter may also be affected by it. Based on this thought and on the bi-directional leader model, the effect of regional ground altitude on lightning striking distance was investigated. The result shows that the striking distance increases significantly as the ground altitude increases. This is because the critical electric field necessary for sustaining the negative streamer zone decreases as the ground altitude increases. The result is useful to both physical and engineering application.

Keywords: leader potential, lightning striking distance, return stroke, ground altitude

1 INTRODUCTION

In negative cloud-to-ground flashes, the first return stroke is always initiated by a stepped leader that travels from the cloud to the ground. As the stepped leader descends to tens to hundreds of meters above ground, the charge in the leader channel will generate a relatively large electric field in front of the leader tip leading to an electric breakdown between the leader tip and the ground or objects connected to it. This final breakdown is usually referred to as the lightning attachment, and the height of the leader tip above the ground at which the lightning attachment starts is usually referred to as the "striking distance". Obviously, it is this lightning attachment that determines the lightning striking point on an object to be struck, making the striking distance the most important parameter in lightning protection issues.

Usually the lightning attachment process, which determines the striking distance, may involve an upward connecting leader from the ground or grounded objects. Due to this, many existing striking distance models have paid more attention to the criterion for upward leader inception, such as critical radius concept [1-2], critical potential criterion [3-4], critical streamer length criterion [5], and leader stabilisation field concept [6-8]. However, if the ground is completely flat, once the corona steamer from the stepped leader tips touches the ground, the final breakdown will take place before or without any initiation of upward connecting leader. In such case, the striking distance was evaluated by the length of the negative streamer region when it reaches the ground. In fact, even if a positive upward connecting leader (for negative cloud-to-ground flashes) is successfully incepted from the ground or a structure (for ordinary ground structures), it starts slowly and moves continuously, and does not have too much time to develop [9]. As a result, it has no more influence on the development of a downward stepped leader and therefore has less importance for striking distance.

Traditionally, the striking distance has been correlated with the prospective return stroke lightning peak current and further, with the geometric parameter of the grounded structure [5, 10-11]. However, many studies show that the striking distance is determined mainly by the last step length of the downward leader near the ground [12-14], which can be estimated with both the leader tip potential just before it touches the earth and a constant critical electric field along the negative streamer region in front of the leader tip. Thus, the leader tip potential is believed by those studies to be a dominant factor affecting leader interaction with a grounded structure. In some studies [4, 13-16], the leader is assumed to be a conducting wire extending in the ambient electric field of a thundercloud, thus, the leader potential is largely controlled by the potential profile of the cloud, the point of leader initiation and the shape of leader path.

The critical electrical field sustaining the streamer zone propagation varies with the air pressure and water vapour content, therefore may vary with the regional altitude above sea level. Phelps and Griffiths in [17] studied the effects of the pressure and humidity on the critical electric field for the positive steamer propagation and further on the striking distance. However, the effects of regional altitude on the critical electric field in the downward negative streamer in front of the downward leader tip, on the potential of the leader tip, and further on the striking distance have not been addressed yet.

In this paper, by using a triple cloud charge model and a bidirectional leader model in combination with the leader potential concept of striking distance [14], the effect of the regional altitude on the striking distance is mainly investigated.

2 MODEL DESCRIPTION

2.1 Tripole structure of the cloud charge

It has been recognised that the charge structure allowing a flash to emerge from the thundercloud is the typical tripole structure: a dominant negative charge in the middle of the cloud, a positive charge above it and a (usually small) positive charge below. The lower positive charge is essential for the initiation of negative cloud-to-ground lightning [18-20]. Although the electrical structure of thunderstorms may be more complex, the potential profile in a thunderstorm is typical and quite stable, and is consistent with a simple dipole or tripole charge model [21].

In particular, the charge configuration used in this study is similar to the modified tripole charge model in [15]. The charge model is consisted of a dominant dipole and a small high charge density core enclosed at the lower part of the main negative charge region. The core corresponds to an intensive updraft region, which is split in two: a small positive charge core and a small negative charge core (see Fig.1). Where the parameter H stands for the altitude of boundary between the two small charge cores, h the ground altitude above sea level, h' the height of the cloud base above ground, and $h_1\lambda$, $h_2\lambda$ and $h_1\lambda$ the layer depth of the small positive charge core, the small negative charge core, and the upper positive charge region, respectively. Among these, h_1 = 3 km, h_2 =4 km, and λ is a zoom factor of the depth of charge regions. For selected parameters H, h and λ, the profile of potential U and vertical electrical field E along the axis of the model are obtained by integrating the disk charge.

Fig.2 shows the profile of U and E for the model for H = 7 km, h = 2 km and λ = 1. There are two competed maximum fields at boundaries between the two opposite charge regions. The lower one, which is closely associated with the presence of the lower positive charge region, is crucial to the initiation of the negative cloud-to-ground discharge.

2.2 Bidirectional leader development

For the development of lightning leader, the concept of the bidirectional lightning leader model, which is widely accepted in the interpretation of a variety of physics processes of lightning in [15, 22-25], was employed. The essence of the concept is: lightning development in cloud occurs as a bi-directional, bipolar, zero-net-charge leader and as an electrodeless discharge [26-29]. In a simple one-dimension bi-directional model in [15], the leader channel was assumed to be a perfect thin conductor that develops vertically downward and upward from the initiation point with constant speed. The leader potential was determined by the average ambient potential along the conductor length. A similar approach was used in [30] to investigate the evolution of initial leader velocities during intra-cloud lightning. Instead of using the constant velocity, they considered the self-consistent evolution of the leader. In principle, the leader propagation model in this study is a combination of those in [14-15] and [30], however, the potential gradient in the leader channel is considered, in addition, the streamer zone in front of the leader tip is also included.

Studies of positive spark in long air gap show that the propagation of the leader channel involves a corona zone at its head [31-33]. The leader channel advancement acts as a metallic electrode, sustaining the field at the front of the leader head for continuous breakdown. The active ionisation at the front of the leader head supplies the current and energy input necessary to sustain the thermal transition at the leader head for its extension. There is apparent asymmetry between positive and negative leaders. The propagation of negative leader is harder to initiate, more intermittent and stepwise. However, in consideration of the evolution of negative leader within a given step, we assume the leader for positive and negative is similar, both propagating with corona at their head, which is characterised by a constant critical electric field E_s [12, 31-33]. The length of the corona can be evaluated by the geometric construction as the length between the leader tip and the point defined by the intersection of the ambient potential curve with a straight line of slope E_s in corona.

There is pressure dependence for the critical breakdown or breakdown field in the atmosphere [5, 38-39]. Assume the same relation for the critical field for both the positive and negative streamer zone, it gives

$$E_s = E_{s0} \exp(-z / z_0), \tag{1}$$

where, z_0 is a constant of 8.4 km, z the height above sea level, E_{s0} the critical field at sea level which is assumed to be 5.0 kV/cm and 7.5 kV/cm for positive polarity and negative polarity, respectively.

It is believed that the leader is consisted of a thin conducting core surrounded by a corona envelope of tens of meters in diameter. To calculate the electric field to find the steamer zone in front of the leader tip, it is first necessary to specify the leader charge distribution within the corona sheath along the channel, which is governed by the leader potential and the ambient potential. The leader, however, is usually with a potential gradient along its channel to maintain a current to sustain the leader extension. To estimate the potential gradient in the leader channel, the semi-empirical model proposed by Bazelyan and Raizer in [4] is adopted, in which the leader tip speed, leader tip current and the leader potential gradient are controlled by the potential difference ΔU_{tip} between the potential of the leader tip and the ambient potential at the edge of the corona zone (also see [36]). In their model, the average leader speed is given as

$$v_L = a(\Delta U_{tip})^{1/2}, \qquad a = 15 mV^{-1/2}s^{-1}. \tag{2}$$

The average leader tip current i_L is then related to v_L and the leader tip charge density τ_L by

$$i_L = \tau_L v_L = \tau_L a(\Delta U_{tip})^{1/2}. \tag{3}$$

Because of the negative current-voltage characteristic of the leader channel, the longitudinal electrical field (potential gradient) in the channel is related to the channel current by

$$E_L = \frac{b}{i_L}, \quad b = 3\times10^4 VAm^{-1} \quad . \tag{4}$$

For a leader that grows steadily, the electric field in its channel core E_L must not be stronger than the undisturbed external field E_0, $E_L \le E_0$. Related to (4), the leader survival condition is

$$i_L \ge \frac{b}{E_0} \quad . \tag{5}$$

With the potential gradient of the leader channel E_L and the potential of the middle point of the leader channel φ_0, the leader potential along the leader channel $\varphi(z)$ is readily obtained, then the charge density in the leader channel can be calculated.

In calculation of the charge density in the leader channel, instead of the method in [12], the charge simulation method in [37-38] is employed. The major reason is that the method of charge density in [12] is sensitive to the radius of the corona sheath of the leader channel assumed, while the charge simulation method in [37-38] is not. At a moment during the leader development, the channel of leader is divided into *N* segments; each segment is assumed a uniformly charged cylinder. Let τ_i be the charges per unit channel length of the *i*-th segment, the leader potential $\varphi(z_k)$ at given point z_k along the leader-streamer channel and below it is written as

$$\sum_{i=1}^{N} \alpha_{ki}\tau_i + U(z_k) = \varphi(z_k), \tag{6}$$

where, $U(z_k)$ is the undisturbed ambient potential due to the thundercloud for the point z_k, and

$$\alpha_{ki} = \frac{1}{4\pi\varepsilon_0 R^2}[(z_{i2}-z_k)(\sqrt{(z_{i2}-z_k)^2+R^2}-|z_{i2}-z_k|)-(z_{i1}-z_k)(\sqrt{(z_{i1}-z_k)^2+R^2}-|z_{i1}-z_k|)$$

$$+R^2\log\frac{z_{i2}-z_k+\sqrt{(z_{i2}-z_k)^2+R^2}}{z_{i1}-z_k+\sqrt{(z_{i1}-z_k)^2+R^2}}] \tag{7}$$

is a potential coefficient of the *i*-th segment relating to the point z_k, z_{i2} and z_{i1} are the coordinates of the ends of the *i*-th segment of the leader channel, and *R* is the radius of the charged leader channel. As shown by Eq. (7), the α_{ki} is not sensitive to the *R* unless the segment z_i is very close to the point z_k concerned.

A summary of the leader channel radius can be found in the work by Vargas [25], in which it says the leader channel radius ranges from 0.5 m to 5 m. From photographic measurements in South

Africa, Schonland [39] reported luminous stepped-leader radius between 0.5 - 5 m. In [12, 14], Mazur proposed that the radius of the leader channel is related to its charges and hence to its potentials. A leader with a potential of -10 MV and -40 MV would have a channel radius of about 1 m and 5 m respectively. In [40], Cooray pointed out that the radius of the leader channel corresponding to a charge density of -0.001 C/m would be about 3 m. All these also suggest that the leader radius may change with its charges and potentials. The larger the leader potential is the lager of its radius. A leader radius smaller than its actual value may lead to underestimation of its charge on one hand, and on the other hand it may lead to the calculated E-field within the leader sheath exceeding the air breakdown electric field which is against the definition of the leader sheath radius.

Referring to [12, 14], as the leader potential involved in this paper is up to more than 90 MV, the corresponding leader radius should be larger than 5 m. But taking account of the upper limit of the observed leader radius by Schonland, we use 5 m as the leader radius in this paper. In fact, since the leader charge is axis-symmetrically distributed along the leader channel, different leader radius should make no more difference in the potential profile along the thin leader core and out of the leader sheath, and hence it has no more influence on the calculation of the strike distance that is based on the leader core potential. But it does little difference in the charge distribution within the leader sheath. To examine the sensitivity of the striking distance to the leader radius, for the case of H=7km, h=2km and λ=1, the evolutions of leader charge density and leader potential profile have been calculated and compared for leader radiuses of 3 m and 5 m. The results show that the charge density for the leader radius of 3 m is smaller than that for the leader radius of 5 m by less than 5%. Meanwhile, the potential profiles for the leader radiuses of 3 m and 5m are almost the same.

Eq. (6) is written for all selected points of the bi-polar leader channel. The set τ_i are solved with the least square error method [38] in such a way that the potential at the middle point of the leader channel φ_0 (therefore the leader channel potential $\varphi(z_k)$) is adjusted so that the total charge induced in all segments of the bipolar leader is zero,

$$\sum_{i=1}^{N} \tau_i \Delta d_i = 0 \quad , \tag{8}$$

where Δd_i is the length of the i-th segment of the leader channel.

Once the line charge density along the leader channel $\tau(z)$ is obtained with the aforementioned charge simulation method, the total charge deposit in part of the leader channel is given by

$$Q = \int_{z_1}^{z_2} \tau(z) dz \, , \tag{9}$$

where z_1 and z_2 are the altitude of the lower end and upper end of the leader channel concerned.

Particularly, the charge deposited in the downward negative leader Q_1 can be estimated using Eq. (9) by setting z_1 as the lower negative leader tip and z_2 as the center sign reversal point of the bidirectional leader channel. Similarly, the charge deposited in the upward positive leader Q_2 can be estimated using Eq. (9) by setting z_1 as the center sign reversal point of the leader and z_2 the upper positive leader tip. As the leader channel is zero-net-charge, the charge deposited in the downward negative leader Q_1 is equal to that in the upward positive leader Q_2. The current at the center charge sign reversal point of the leader channel, i_0, is given by

$$i_0 = \frac{dQ_2}{dt} = -\frac{dQ_1}{dt} \quad . \tag{10}$$

When the negative streamer zone in front of the leader tip reaches the ground, the striking distance with respect to flat ground is then obtained as the streamer length [12] by

$$S = \phi / E_{sg} , \tag{11}$$

where Φ is the leader tip potential just before it touches the ground and E_{sg} is the critical field for the negative streamer zone at ground level.

In deriving the above leader model, several assumptions for simplification were made, which are discussed below:

1) The tortuousity and branching are neglected, which may lead to over-estimation of the striking distance according to [11] and [25], due to the over-estimation of the leader potential [4, 15]. In addition, the tortuousity and branching may be associated with the stochastic behaviour of the lightning striking point. Since the effects of those factors are unknown and debatable, neglecting them is justifiable.

2) The other atmospheric conditions, such as temperature and humidity are not considered.

3) Instead of the step transient speed of negative stepped leader, the step average speed is introduced to describe the extension of leader within a step. In practice, the striking distance, which is dominated by the leader tip potential, is also affected by the step-wise behaviour of the leader just before the attachment, with the length of the last step being its upper limit. What is calculated based on Eq. (11) and by using the step average speed is actually the maximum striking distance with the influence of step-wise behaviour on the striking distance being ignored. To estimate leader tip potential with a high accuracy, the increment of the leader channel extension (or time step) in the numerical calculation should be much smaller than the step length. In this study, by numerical testing, a time step of 50 μs subjecting to Eq. (2) is considered to be adequate.

4) The semi-empirical model (Eq. (2) to Eq. (5)) derived by Bazelyan and Raizer [4] for positive leaders under switching impulse voltages are extrapolated to the negative leaders under atmospheric conditions. This rough extrapolation may introduce errors in estimates of leader potential gradients via the leader speeds and currents; furthermore it may affect the accuracy of the estimated leader tip potential and therefore the estimated striking distance. Fortunately, the leader potential is largely controlled by the ambient potential profile. The leader potential gradient is just a small factor in determining the leader tip potential.

3 RESULTS AND ANALYSES

3.1 Evolution of the leader

It is assumed that a cloud-to-ground lightning is initiated at the altitude of H where the electric field is the maximum, and the leader channel has an initial length of L = 1 km with an initial potential gradient along the channel of 1 kV/m and grows in a 50 μs time step. For the simulation in a step (say step n), with the leader channel length, the leader speed and the leader channel potential gradient calculated in the previous step (step $n-1$), the charge distribution (τ) along the leader channel for the step n can be estimated based on Eq. (6), (7) and (8). With the recalculated charge distribution, the ambient potential profile for the step n can be recalculated. Consequently, the leader tip speed (v_L, subject to Eq. (2)), the leader tip currents (i_{bottom} and i_{top}, subject to Eq. (3)) and the leader potential gradient (E_L, subject to Eq. (4)) for the step n can be estimated. The recalculated leader speed and leader potential gradient for the step n can then be used for the simulation in the next step (step $n+1$). The ambient potential profile below the leader tip is calculated as the undisturbed cloud-produced potential plus the potential due to the leader channel charges by Eq. (6). In addition, Eq. (5) is tested in each step. If Eq. (5) is fulfilled, then go to the next step, otherwise, the leader stops.

Fig.3 shows the evolution of potential profile along the bidirectional leader-streamer channel at a 6.5 ms time interval for the case H = 7 km, h = 2 km and λ = 1, based on the charge simulation method with the cloud charge model shown in Fig.1. The result is similar to that in [15], but different in the following two points. First, we have considered the potential gradient along the leader channel. Second, we have considered the streamer zone in front of the leader tip. The potential distribution in the streamer zone is characterised with a straight line of a slope of the critical electrical field E_s. The length of the streamer zone is determined as the distance between the leader tip and the point defined by the intersection of the ambient potential curve with a straight line of slope E_s in the streamer zone.

Fig.4 shows the evolution of the induced charge profile along the leader channel corresponding to Fig.3, calculated based on the charge simulation method. It can be seen that the charge densities at the leader tips usually show a sharp increase due to the "electrode tip" effect. For the upper positive leader part, the charges are mainly concentrated at the height of H = 7 km, where the main negative charge region of the cloud is, while the charges are mainly concentrated near the tip for the lower negative leader part. This feature is consistent with the ambient potential distribution shown by the dot-line in Fig. 3, as the charge on the leader channel is induced due to the ambient potential.

Fig.5 demonstrates the evolution of the current at the two ends of the leader channel and that at the leader center corresponding to Fig.3 and Fig.4. It can be seen that the upward positive leader current initially increases and then decreases to the minimum, while the current at the negative end increases steadily when it approaches to the ground. This is in accord with the variation of potential difference at the leader tip ΔU_{tip} (see Fig.3) and the variation of charge density along the leader channel (see Fig.4). The center current is less than a hundred ampere, which agrees with the result of others [4, 14].

3.2 Striking distance variation with ground altitude

In investigating the striking distance variation, three parameters, H, h and λ were used to adjust the charge structure. It is believed that the initiation of cloud-to-ground lightning always occurs at the same height as the boundary between the mid-level negative and lower positive charge regions, where it is corresponding to the charge reversal temperature of about -10 to -20 ºC [40]. Starting from this basic point of view, following case studies are introduced.

Case 1 – Since the cloud temperature is dependent with the altitude above sea level, thus, as Case 1, it is assumed that the leader initiation altitude remains as a constant at H = 7 km with λ = 1. Changing the altitude of the ground h and the cloud base height h', the variation of the striking distance with altitude of the ground h is then obtained as shown in Fig.6. It can be seen that the striking distance increases as the altitude of the ground h increases. This is expected by Eq. (1) and Eq. (11) as the critical field of the negative streamer at ground level exponentially decreases with the increase of the ground altitude, while the leader potential changes in a narrow range of 90 to 93 MV as the ground altitude varies.

Case 2 – In addition to the leader initiation altitude, the variation of potential profile with the ground altitude also affects the striking distance. To investigate this effect, as Case 2, the height of the cloud base to ground (h' = 2 km with $\lambda = 1$) remains as a constant while the ground altitude h changes. In such case the cloud background potential remains invariant and the striking distance is only affected by the critical field. Similar calculations is also repeated for h' = 0.5 km with $\lambda = 1$, which is referred as Case 3. The result of Case 2 is similar to that of Case 1, while there is a less than 10 m difference in striking distance between Case 2 and Case 3.

In the above cases, the variation of cloud charge structure with charge region altitudes is not taken into account. However, both theoretical and experimental works show that the electric field within cloud is limited by the critical field of lightning initiation. According to this, the electric field at the leader initiation altitude should remain invariant regardless of the change of the ground altitude. Therefore, as Case 4, all other things are the same as Case 1, except the zoom parameter λ. With the increase of ground altitude h, the λ is adjusted so that the electric field at lightning initiation height remains the same as the case when the ground altitude is at sea level. Fig.7 shows the comparison of striking distance between Case 1 and Case 4. It can be seen that with the increase of the ground altitude, the thunderstorm charge may become weaker ($\lambda < 1$), and the striking distance may decrease also. However, the difference is less than 13 m between the two cases.

3.3 Leader charges and return stroke charge transfer and striking distance

The leader tip potential that determines the striking distance is highly associated with the ambient potential profile. On the other hand, the charge stored on the negative leader channel is also highly associated with ambient potential profile. Therefore, the striking distance may be associated with the charge stored on the downward negative leader channel. Some engineers are also like to associate the striking distance with the total charge induced in the channel of the return stroke just following the downward leader, as the total charge induced in the return stroke channel is theoretically associated with the ambient potential profile too. But the problem is that the return stroke occurs after the attachment from the striking distance, while the leader potential and its charges precede the attachment. So, from the point of view of physicists, only the relationship between the leader charges and the striking distance makes sense to them.

For the bidirectional leader in this study, the total return stroke charge transfer Q is equivalent to the positive charge induced in the whole bidirectional leader channel by the cloud charge after the leader touches the ground, which can be easily calculated by setting the leader channel potential $\varphi(z_k)$ to the ground potential in Eq. (6) based on the charge simulation method. The negative charge stored in the downward negative leader channel just before touching the ground is referred as Q_1, which can be estimated based on Eq.(9) given that the charge distribution along the leader channel is obtained.

Fig.8 shows the variation of the charge stored on the negative leader channel before touching ground Q_l, and the total return stroke charge transfer Q, against the striking distance S, when the ground altitude changes from 0 to 3.0 km with H = 7 km and λ = 1. It shows that the charge stored on the negative leader channel decreases with the increase of striking distance (or the ground altitude). This is understandable as the length of the leader channel decreases with the increase of ground altitude, so does the charge associated with the leader channel.

To further investigate the effect of ground altitude on the relationship between the striking distance and the charge stored on the negative leader channel, the following study is done.

First, fix the ground altitude h but change the parameter λ, so that both the striking distance S and the charge stored on the negative leader channel Q_l are changed. A relation between the S and Q_l is then obtained by curve fitting with a formula as

$$S = kQ_l^{\,v}. \tag{12}$$

Secondly, repeat the above process for different ground altitudes h ranging from 0 to 2km, a series of S - Q_l curves are obtained as shown in Fig.9. It is found that both the parameters k and v in Eq. (12) are changed with the change of ground altitude h. The k increases from 54 to 89 while the v increases from 0.96 to 0.87, when the h increases from 0 to 2 km. This result can be specified as

$$S = (54 + 17.5h)Q_l^{(0.96-0.045h)}, \tag{13}$$

where h is the ground altitude above sea level in km.

In engineering practice, the striking distance S is conventionally related to the peak current of the first return stroke I as

$$S = aI^{b}. \tag{14}$$

where, a and b are two constants. And in many studies [41-42], the peak current of the first return stroke is associated with the total charge transferred to the ground by the return stroke excluding the continuous current. However, Mazur and Ruhnke in [14] have shown that correlation between the leader potential (which determines the striking distance) and the peak return stroke current is extremely weak. The return stroke is affected by both, the features of the preceding leader as well as by characteristics of the grounding system of the object. The firm association of the peak current to the total charge transfer by the return stroke is questionable unless the waveforms of every return stroke are the same for every cloud-to-ground flash.

4 CONCLUSION

In this work, a simple self-organised propagation model of bi-directional leader heading by a streamer zone was employed to discuss the possible effect of the ground altitude on the lightning striking distance. The model, which is a further development of that of Mazur and Ruhnke [13-15] and Behnke et al. [30] with a streamer zone in front of the leader tip and with the charge simulation method [37-38], enables the calculation of many parameters of the channel, such as the charge distribution along the leader channel, leader current, leader potential, and the striking distance to flat ground. The main parameters obtained, such as the leader charge distribution and the leader current, are in agreement with previous results. Based on the leader tip potential concept of striking distance, the effects of regional ground altitude on the striking distance was investigated. It shows that the striking distance increases significantly with the increase of the regional ground altitude mainly due to the decrease of the critical electric field necessary for sustaining the negative streamer zone.

ACKNOWLEDGMENTS

The work leading to this paper is supported by Research Committee of The Hong Kong Polytechnic University and Research Grant Council of Hong Kong Government (Grants No.: PolyU-512908E). The authors would like to thank the two anonymous reviewers for providing valuable comments on the paper.

REFERENCES

[1] Eriksson, A. J. (1987), An improved electro-geometric model for transmission line shielding analysis, *IEEE Trans. Power Deliv.*, 2(2), 871–886.

[2] Dellera, L. and E. Garbagnati (1990), Lightning stroke simulation by means of the leader progression model: I. Description of the model and evaluation of exposure of free-standing structures, *IEEE Trans. Power Deliv.*, 5, 2009–2022.

[3] Rizk, F. (1994), Modeling of lightning incidence to tall structures, part I: Theory, *IEEE Trans. Power Deliv.*, 9, 162–171.

[4] Bazelyan, E. M. and Y. P. Raizer (2000), Lightning Physics and Lightning Protection, *Institute of Physics Publishing: Philadelphia.*

[5] Petrov, N. I. and R. T. Waters (1995), Determination of the striking distance of lightning to earthed structures, *Proc. R. Soc. A.* 450, 589–601.

[6] Lalande, P., A. Bondiou-Clergerie, G. Bacchiega, and I. Gallimberti (2002), Observations and modeling of lightning leaders, *C.R. Phys.*, 3, 1375–1392.

[7] Becerra, M. and V. Cooray (2006), A simplified physical model to determine the lightning upward connecting leader inception, *IEEE Trans. Power Deliv.*, 21, 897– 908.

[8] Cooray, V. and N. Theethayi (2007), The striking distance of lightning flashes, and the early streamer emission (ESE) hypothesis, *J. Electrostatics*, 65, 336–341.

[9] Cooray, V. (2010), Non Conventional Lightning Protection systems, *30th International Conference on Lightning Protection*, Cagliari, Italy, Sep. 13-17, 2010.

[10] Haddad, A. and D. F. Warne (2004), Advanced in High Voltage Engineering, Ch.3, *The Institution of Electrical Engineering, London, United Kingdom*.

[11]Cooray, V., V. Rakov, and N. Theethayi (2007), The lightning striking distance: Revisited, *J. Electrostatics.*, 65(5– 6), 296– 306.

[12] Mazur, V., L. H. Ruhnke, A. Bondiou-Clergerie, and P. Lalande (2000), Computer simulation of a downward negative stepped leader and its interaction with a ground structure, *J. Geophys. Res.*, 105, 22,361– 22,369.

[13] Mazur, V. and L. H. Ruhnke (2002), Determining leader potential in cloud-to-ground flashes, *Geophys. Res. Lett.*, 29(12), 1601, doi:10.1029/2001GL014159.

[14] Mazur, V. and L. H. Ruhnke (2003), Determining the striking distance of lightning through its relationship to leader potential, *J. Geophys. Res*., 108(D14), 4409, doi:10.1029 /2002JD003047.

[15] Mazur, V. and L. H. Ruhnke (1998), Model of electric charges in thunderstorms and associated lightning, *J. Geophys. Res*., 103, 23,299 –23,308.

[16] Aleksandrov N. L., E. M. Bazelyan and Y. P. Raizer (2005), Initiation and development of first lightning leader: the effects of coronae and position of lightning origin *Atmos. Res.* 76, 307–29.

[17] Phelps, C. T. and R. F. Griffiths (1976), Dependence of positive corona streamer propagation on air pressure and water vapor content. *J. Appl. Phys*. 47, 1929-1934.

[18] Clarence, N. D. and D. J. Malan (1957), Preliminary discharge processes in lightning flashes to ground, Q. *J. R. Meteorol. Soc.*, 83, 161–172.

[19] Williams, E. R. (1989), The tripole structure of thunderstorms, *J. Geophys. Res.*, 94 (D11), 13,151–13,167.

[20] Williams, E. R. (2008), Atmospheric science - Predictable lightning paths? *Nature Geosci.*, 1(4), 216-217.

[21] Stolzenburg, M. and T. C. Marshall (2008), Serial profiles of electrostatic potential in five New Mexico thunderstorms, *J. Geophys. Res.*, 113, D13207, doi:10.1029/2007JD009495.

[22] Mansell, E. R., D. R. MacGorman, C. L. Ziegler, and J. M. Straka (2002), Simulated

three-dimensional branched lightning in a numerical thunderstorm model, *J. Geophys. Res.*, 107(D9), 4075, doi:10.1029/2000JD000244.

[23] Tan, Y. B., S. C. Tao and B. Y. Zhu (2006), Fine-resolution simulation of the channel structures and Propagation features of intracloud lightning, *Geophys. Res. Lett.*, 33, L09809, doi: 10.1029/2005GL025523.

[24] Riousset, J. A., V. P. Pasko, P. R. Krehbiel, R. J. Thomas, and W. Rison (2007), Three-dimensional fractal modeling of intracloud lightning discharge in a New Mexico thunderstorm and comparison with lightning mapping observations, *J. Geophys. Res.*, 112, D15203, doi:10.1029 /2006JD007621.

[25] Vargas, M. and H. Torres (2008), On the development of a lightning leader model for tortuous or branched channels, *J. Electrostatics*, 66(9-10), 482–495.

[26] Kasemir, H. W. (1960), A Contribution to the Electrostatic Theory of a Lightning Discharge, *J. Geophys. Res.*, 65(7), 1873–1878.

[27] Mazur, V. and L. H. Ruhnke (1993), Common physical processes in natural and artificially triggered lightning. *J. Geophys. Res.*, 98, 12913-12930.

[28] Mazur, V. (2002), Physical processes during development of lightning flashes, *C. R. Physique*, 3, 1393-1409.

[29] Williams, E. R. (2006), Problems in lightning physics - the role of polarity asymmetry *Plasma Sources Sci. Technol*. 15 (2), S91- S108.

[30] Behnke, S. A., R. J. Thomas, P. R. Krehbiel, and W. Rison (2005), Initial leader velocities during intracloud lightning: Possible evidence for a runaway breakdown effect, *J. Geophys. Res.*, 110, D10207, doi:10.1029/2004JD005312.

[31] Bondiou A. and I. Gallimberti (1994), Theoretical modeling of the development of the positive spark in long gaps, *J. Phys. D: Appl. Phys*, 27, 1252–1266.

[32] Goelian N., P. Lalande, A. Bondiou-Clergerie, G. L. Bacchiega, A. Gazzani, and I. Gallimberti, (1997), A simplified model for the simulation of positive spark development in long air gaps, *J. Phys. D: Appl. Phys.*, 30, 2441–2452.

[33] Gallimberti, I., G. Bacchiega, A. Bondiou-Clergerie, and P. Lalande (2002), Fundamental processes in long air gap discharges, *C.R. Phys.*, 3, 1335–1359.

[34] Dwyer, J. R. (2003), A fundamental limit on electric fields in air, *Geophys. Res. Lett*., 30(20), 2055, doi:10.1029 /2003GL017781.

[35] Marshall, T. C., M. P. McCarthy and W. D. Rust (1995), Electric field magnitudes and lightning

initiation in thunderstorms, *J. Geophys. Res*., 100, 7097– 7103.

[36] Bazelyan, E. M., Y. P. Raizer and N. L. Aleksandrov (2008), Corona initiated from grounded objects under thunderstorm conditions and its influence on lightning attachment, *Plasma Sources Sci. Technol*. 17, 1–17.

[37] Singer, H., Steinbigler, H. and P. Weiss (1974), A charge simulation method for the calculation of high voltage fields, IEEE Trans. PAS 93 1660 – 1668.

[38] Malik, N. H. (1989), A Review of the Charge Simulation Method and its Applications, IEEE Transactions on Electrical Insulation, 24(1), 3-20.

[39] Schonland, B. F. (1953), The pilot streamer in lightning and the long spark, Proc R Soc A, 220, 25-38.

[40] Cooray, V. (2003), The Lightning Flash, *Institution of Electrical Engineers: London*, p 574.

[41] Berger, K. (1972), Methods and results of research on lightning on Mount San Salvatore 1963-1971, *Bull. ASE*, 63, 1403-1422.

[42] Cooray, V. and S. Lundquist (1985), Characteristics of the Radiation Fields From Lightning in Sri Lanka in the Tropics, *J. Geophys. Res.*, 90(D4), 6099–6109.

FIGURES

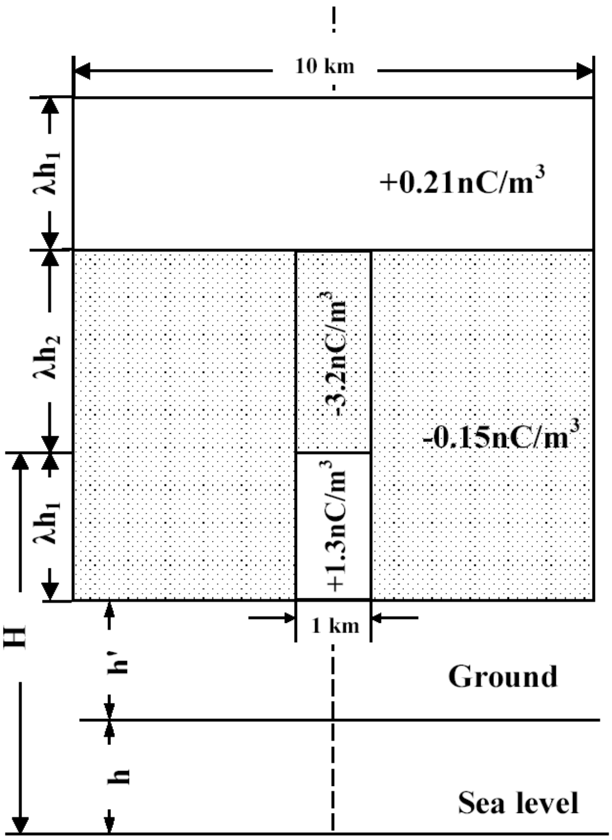

Fig.1 A modified two-dimensional axis symmetrical tripole charge model of a thunderstorm.

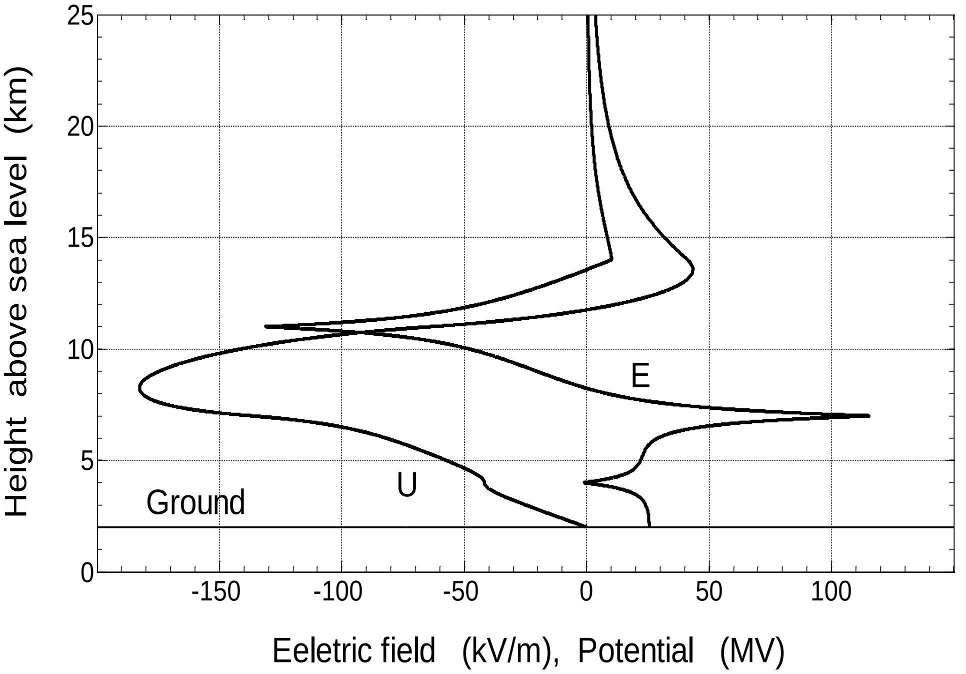

Fig. 2 Profiles of the electric fields and potentials along the axis of the cloud charge model in Fig. 1 for H = 7 km, h = 2 km, λ = 1. U – potentials, E – vertical electric fields.

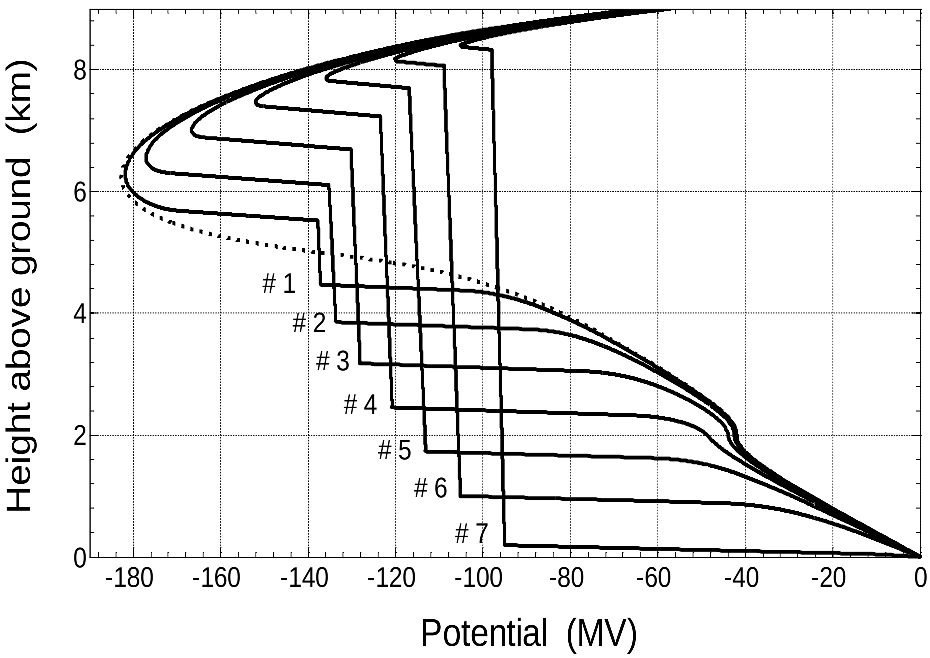

Fig.3 Evolution of the potential profiles on a developing bidirectional leader-streamer system at about 6.5 ms time intervals (solid-lines, indicated by #1, #2 … #7, respectively) with the cloud charge model shown in Fig.1 and the charge simulation method, for H = 7 km, h = 2 km and λ = 1. Dot-line: cloud ambient potential profile as in Fig.2.

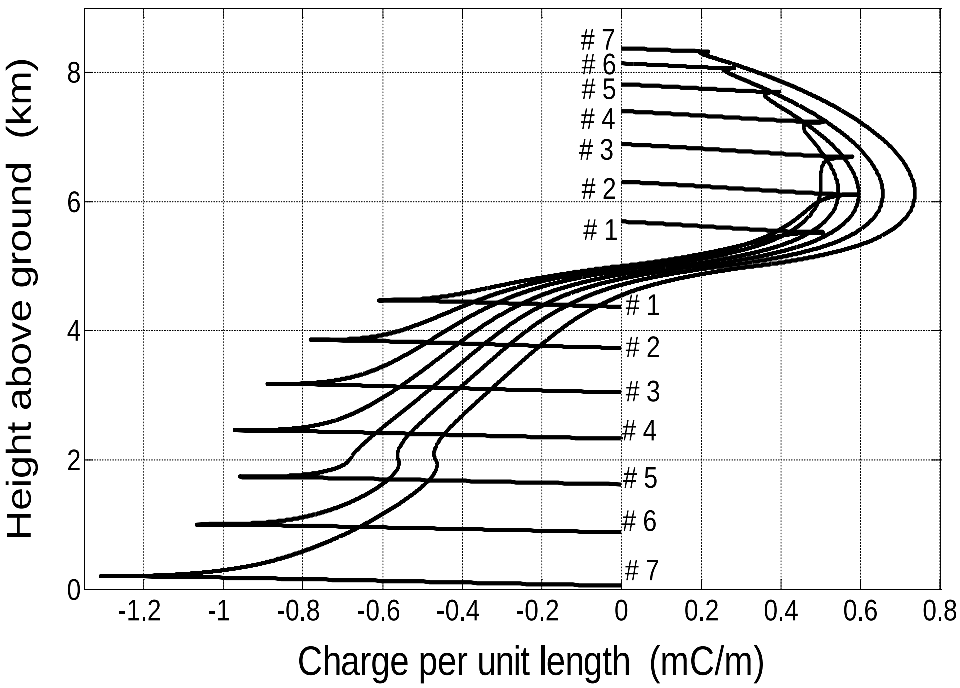

Fig.4 Evolution of the induced charge profiles on a developing bidirectional leader-streamer system at about 6.5 ms intervals (indicated by #1, #2 … #7, respectively) with the cloud charge model in Fig.1 and the charge simulation method, for H = 7 km, h = 2 km, and λ = 1.

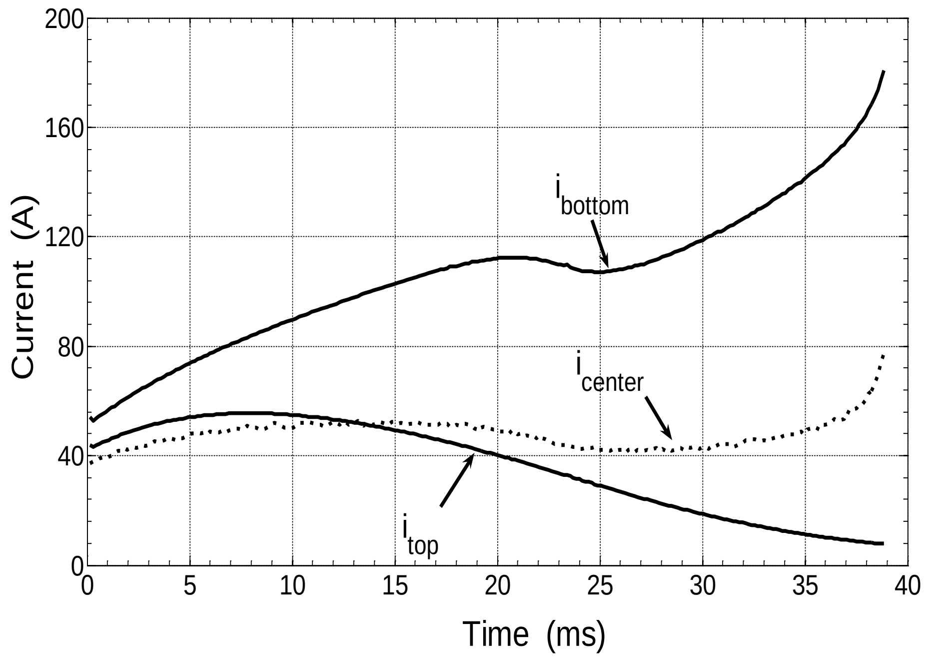

Fig.5 Time variation of the currents at the upper end (i_{top}), bottom end (i_{bottom}) and the center (i_{center}) of the bidirectional leader-streamer system during its propagation as in Fig.4 (H = 7 km, h = 2 km, λ = 1).

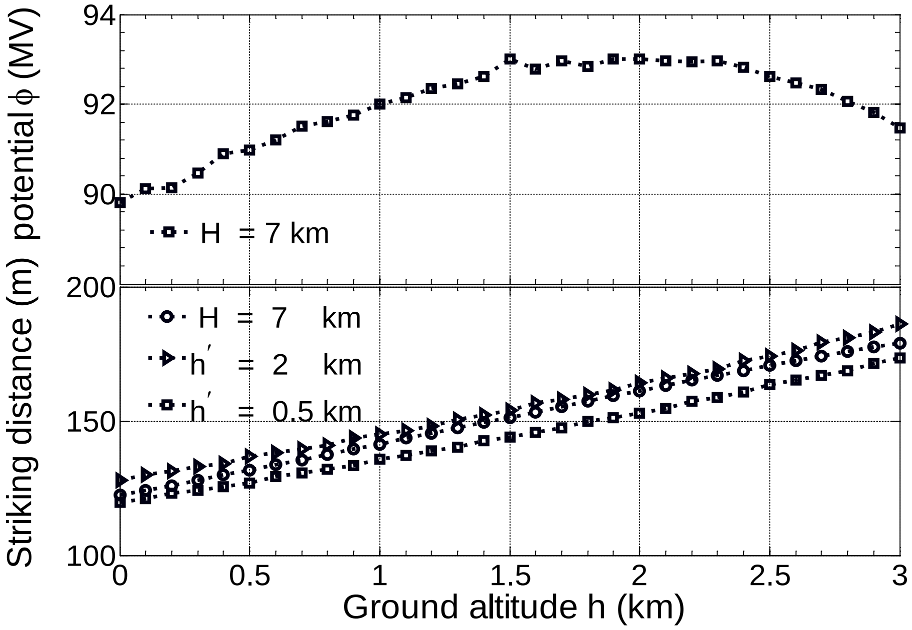

Fig.6 Upper: leader potential before touching ground versus ground altitude for leader initiation height fixed at H = 7 km; Lower: striking distance versus ground altitude for (i) leader initiation height fixed at H = 7 km (circle), (ii) cloud base fixed at h' = 2 km (triangle) and (iii) cloud base fixed at h'= 0.5 km (square), with λ = 1.

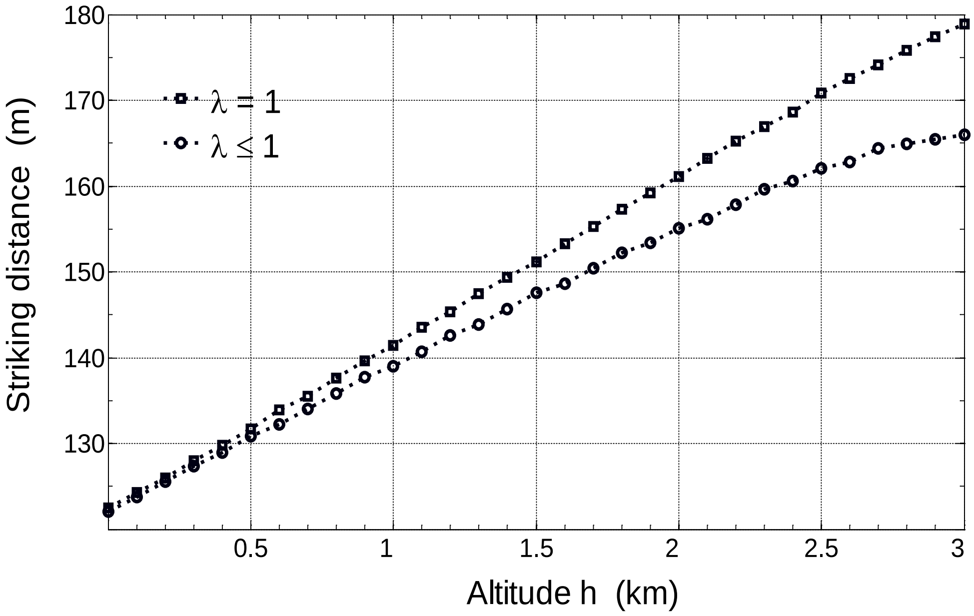

Fig.7 Comparison on striking distance between Case1 (the charge structure unchanged, λ =1) (square) and Case 4 (the electric field at the leader initiation altitude unchanged by adjusting the zoom factor, $\lambda \leq 1$) (circle).

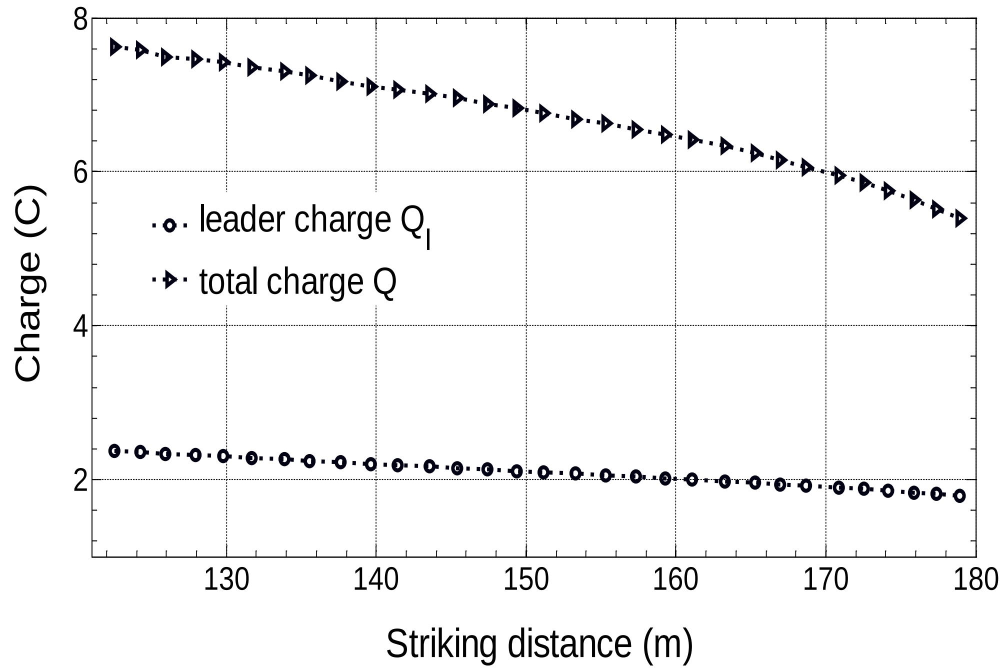

Fig.8 The charge deposit in the negative leader channel before touching ground (Q_l) and the total charge transfer by the return stroke (*Q*).

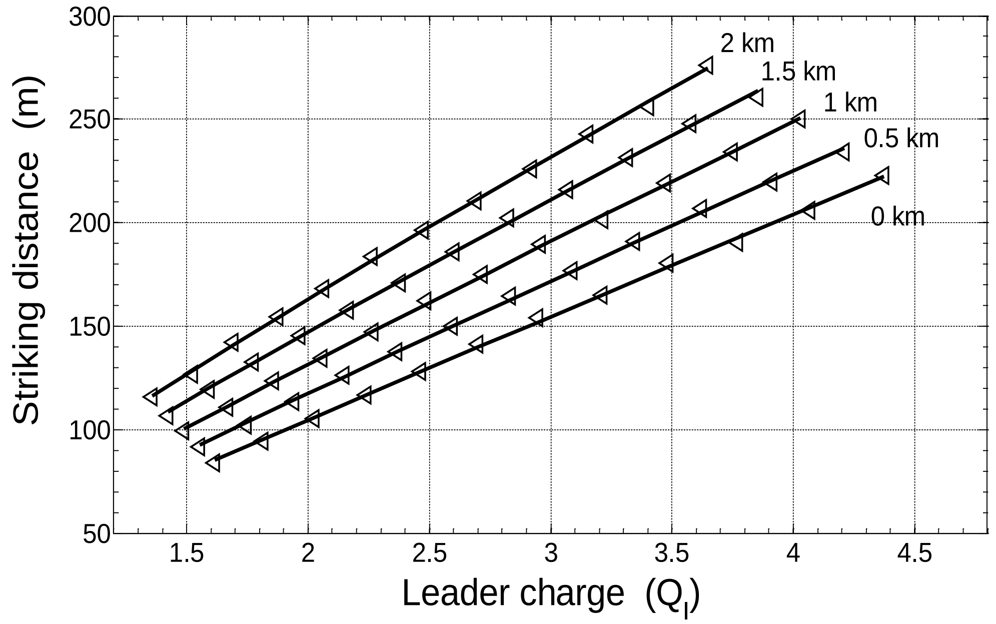

Fig.9 Striking distance versus the charge (in coulomb) stored on the downward negative leader channel for different altitude of the ground *h* changing from 0 to 2 km.